Evaluation of High Step-up Power Conversion Systems for Large-capacity Photovoltaic Generation Integrated into Medium Voltage DC Grids*

Shilei Lu[1], *Kai Sun*[1*], *Haixu Shi*[1], *Yunwei Li*[2] *and Guoen Cao*[3]

(1. Department of Electrical Engineering, Tsinghua University, Beijing 100084, China;
2. Department of Electrical and Computer Engineering, University of Alberta, Edmonton AB T6G2R3, Canada;
3. Institute of Electrical Engineering, Chinese Academy of Sciences, Beijing 100190, China)

Abstract: With the increase of dc based renewable energy generation and dc loads, the medium voltage dc (MVDC) distribution network is becoming a promising option for more efficient system integration. In particular, large-capacity photovoltaic (PV)-based power generation is growing rapidly, and a corresponding power conversion system is critical to integrate these large PV systems into MVDC power grid. Different from traditional ac grid-connected converters, the converter system for dc grid interfaced PV system requires large-capacity dc conversion over a wide range of ultra-high voltage step-up ratios. This is an important issue, yet received limited research so far. In this paper, a thorough study of dc-dc conversion system for a medium-voltage dc grid-connected PV system is conducted. The required structural features for such a conversion system are first discussed. Based on these features, the conversion system is classified into four categories by series-parallel connection scheme of power modules. Then two existing conversion system configurations as well as a proposed solution are compared in terms of input/output performance, conversion efficiency, modulation method, control complexity, power density, reliability, and hardware cost. In-depth analysis is carried out to select the most suitable conversion systems in various application scenarios.

Keywords: Photovoltaic generation, dc-dc conversion, medium voltage dc grid, large-capacity, ultra-high voltage transfer ratio

1 Introduction

In recent years, ac and dc hybrid power distribution networks (shown in Fig. 1) have been found more suitable for the development of modern urban distribution networks due to the following considerations [1-3]: ① A DC grid is more compatible with distributed dc power sources (photovoltaic generation, battery energy storage, etc.) and dc loads (LED lighting, electric vehicles, etc.) with reduced power-conversion losses; ② Voltage stability and power quality of distribution networks can be improved, since the harmonics in ac partitions can be reduced by the dc link; ③ DC cable is a more efficient transmission medium that eases the shortage of urban power transmission corridors. By considering the power capacity and voltage-level requirements of distribution networks, medium voltage dc (MVDC, ⩾10 kV) grids are under rapid development.

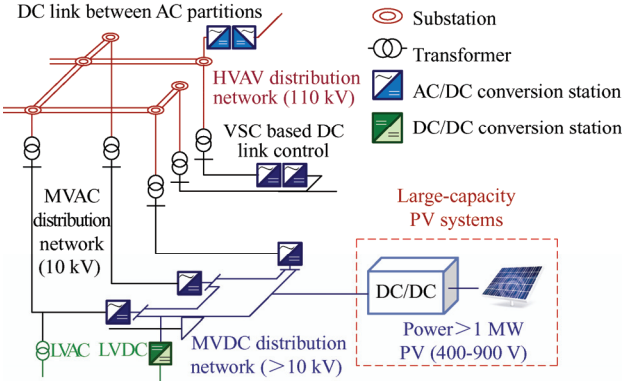

Fig. 1 Large-capacity PV generation integrated into MVDC grids

Renewable energy based power generation, especially photovoltaic generation, also has a rapidly

Manuscript received September 30, 2021; revised November 5, 2021; accepted November 21, 2021. Date of publication December 31, 2021; date of current version December 10, 2021.
* Corresponding Author, E-mail: sun-kai@mail.tsinghua.edu.cn
* Supported by the National Natural Science Foundation of China (51811540405, 52007096) and National Key R&D Program of China (2016YFB0900205).
Digital Object Identifier: 10.23919/CJEE.2021.000033

growing share in global electricity generation [3-6]. Large-scale photovoltaic plants have been successively established worldwide, such as the 1 000 MW photovoltaic industrial park in Gujarat, India, and the 580 MW photovoltaic power plant in Antelope Canyon, Arizona, in the United States. EUMENA plans to install PV plants with 3.3 billion watts of total capacity in the Mediterranean area before 2050, meeting 33% of electricity demand of European countries. The Chinese government plans to increase installed capacity of PV plants to 80 billion watts before 2020. For integrating large-scale and low dc voltage PV energy into a grid, the medium voltage dc grid is a promising choice. These MVDC grid-connected PV systems feature the following advantages over traditional low-voltage ac grid-connected PV systems [7-10]: ① Simple scheme - a dc grid is free from issues of reactive power compensation and harmonic suppression that affect an ac grid; ② Capacity advantage - higher voltage leads to larger capacity, which benefits the economic operation of the system; ③ Efficiency advantage - only dc-dc conversion is required, and the conversion losses are lower than those of multi-stage dc-to-ac (dc-dc and dc-ac) conversion. Also, reactive power losses in ac grids are avoided; ④ Flexibility advantage - the large-capacity renewable power is directly integrated into the MVDC link, which strongly supports the power-flow control of power systems.

The research on large-capacity PV systems integrated into MVDC grids is still emerging, and few system solutions have been proposed. These systems must be thoroughly investigated and studied. Among many kinds of system topologies, the modular parallel-series connected scheme probably is the most promising solution, due to its modular design and low voltage-current stress of components [11-13]. This paper focuses on classification and comparison of these PV integration system solutions based on the modular connection scheme.

The main contributions of this paper are as follows. For large-capacity PV systems integrated into MVDC grids: ① A topological scheme based on a modular parallel-series connection is analyzed and classified. ② A system solution based on compound dc-dc modules is proposed. ③ The proposed system solution and two available system schemes are presented as examples of the classification, and are compared regarding operation performance (by simulation), control strategy, efficiency, device cost, and reliability. ④ How to select the most suitable conversion systems in various application scenarios is discussed. In Section 2, the required features of power-conversion systems for large-scale photovoltaic generation integrated into MVDC grids are investigated. The topological scheme of these systems based on a modular connection is analyzed and classified. In Section 3, three system solutions including the proposed one are introduced. More detailed evaluation and comparison of the three solutions are presented in Section 4. Finally Section 5 concludes the work.

2 Required features and classification of the conversion system

In PV plants, the typical output voltage range of PV arrays is 400-900 V DC. However, the DC link voltages of MVDC grids are usually over 10 kV. Hence a corresponding dc-dc power-conversion system is critical for connecting large-capacity PV arrays to the dc link in MVDC grids.

Considering the demands from both the PV and MVDC grid sides, as shown in Fig. 2, the required features on power-conversion systems for large-scale PV generation integrated into MVDC grids are [14-16]: ① ultra-high voltage step-up ratios (20-50 times); ② wide-range voltage step-up ratios, owing to the need of maximum power-point tracking of PV arrays; ③ unidirectional high power (>1 MW) dc-dc conversion. Moreover, the common goals are to achieve high efficiency, reliability, and stability, and low cost for the power conversion systems.

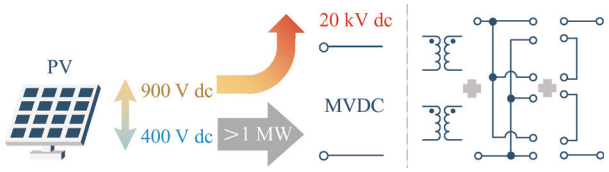

Fig. 2 Requirement and a potential method

To attain the required features, a power-conversion system should have structures with the following characteristics: ① Converter topology is suitable for varying input low voltage; ② The system should consist of multiple modular dc-dc converters with parallel input connections and series output connections (as shown on the right side of Fig. 2), which ensures low voltage and high current on the input side, and high voltage and low current on the output side; ③ Transformer isolation is required in the modular dc-dc converters to realize an ultra-high step-up ratio and galvanic isolation. These characteristics result in a parallel-series connection of modular isolated dc-dc converters. This parallel-series system scheme can easily refer to the well-known input-parallel and output-series modular converters. However, due to the unidirectional high power and voltage levels of large-scale PV integration converters for an MVDC grid, the connection tends to be more complex. Besides parallel-series connections on input and output ports of an entire converter system, inner connections can be necessary.

The most likely location for an inner connection is the primary and secondary sides of each transformer, which means parallel and series connections of the ac link. Combining the connection of the dc link (input and output of the whole conversion system), system connection schemes can be classified. As shown in Fig. 3, the conversion system is divided into six parts by the route of power flows: input dc ports at position ⓐ, primary-side sub-modules, ac ports at position ⓑ, transformers, ac ports at position ⓒ, secondary-side sub-modules (or an entire secondary-side rectifier), and output dc ports at position ⓓ. Ports at ⓐ should be parallel, and ports at ⓑ can be parallel, while for ⓒ and ⓓ, ports in only one position should be series,

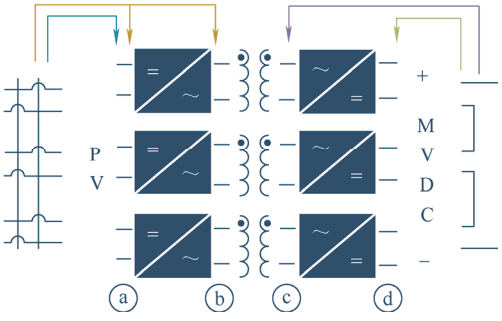

Fig. 3 Possible position for parallel-series connection

since dual series connection causes a short circuit. In particular, when ports at ⓒ are series, secondary-side converter modules between ⓒ and ⓓ merge into a two-port medium-voltage rectifier.

Based on the combination above, four system-connection-scheme categories are derived and presented in Fig. 4.

(1) parallel-distributed-series-rectifier (PDSR).
(2) parallel-parallel-series-rectifier (PPSR).
(3) parallel-distributed-distributed-series (PDDS).
(4) parallel-parallel-distributed-series (PPDS).

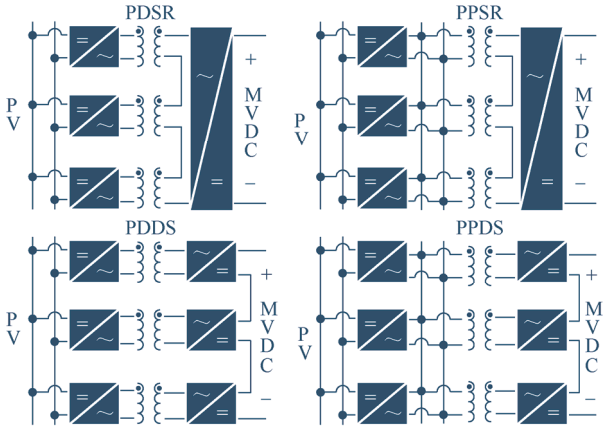

Fig. 4 Four possible categories of system-connection schemes

Different connection positions bring different system features.

PDSR: ① Ports at ⓐ are parallel, while ports at ⓑ are distributed; there is a one-to-one cascading between primary modules and transformers. Hence the number of primary modules must be the same as that of transformers, which decreases the freedom of the transformer design. When a primary module is turned off, its corresponding transformer also stops working, causing system failure. Yet, the power-circulation issue is avoided among primary modules, which simplifies their control and allows a higher working frequency of the transformers. ② Ports at ⓒ are series to produce a medium ac voltage; the secondary modules merge into a rectifier. This multi-level ac voltage is produced by series ports at ⓒ, hence a centralized PWM generator is suitable to facilitate phase-synchronization control of carriers in primary modules. A high-power, high-voltage diode rectifier is capable, though the system is more nonlinear. A multilevel rectifier is another choice to increase power density, system linearity, and response performance,

but at a price of higher device cost and complexity.

PPSR: ① Ports at ⓐ and ⓑ are parallel simultaneously; primary modules are in an input-parallel-output-parallel connection, which produce a common ac bus at ⓑ. Hence the number of primary modules can be different from that of transformers, which increases the freedom of the transformer design. When a primary module is turned off by fault, other parts of the system still work normally. However, the parallel connection at ⓑ can lead to active and reactive power circulation between primary modules, which requires a centralized PWM generator for phase synchronization among modules, and circulation suppressing control or topology. A distributed synchronization scheme goes against transformers working at high frequency. ② Ports at ⓒ are series to produce a medium ac voltage; the secondary modules merge into a rectifier. This ac voltage is not multi-level due to the ac link at ⓑ, hence a sinusoidal voltage rather than rectangular voltage is preferred to minimize the instant voltage-change rate. A high-power, high-voltage diode rectifier is capable, though the system is more nonlinear and efficiency is reduced by diode voltage drops. A multilevel rectifier is another choice to increase power density, system linearity, and response performance, but at a price of higher device cost and complexity.

PDDS: Ports at ⓐ are parallel, while ports at ⓑ are distributed; ports at ⓒ are distributed, while ports at ⓓ are series. There is a one-to-one-to-one cascading among primary modules, transformers, and secondary modules. Hence a primary module, transformer, and secondary module form a super module, with the result that the whole system is implemented by the well-known input-parallel-output-series scheme with a whole modular design. The voltage stress of secondary modules is significantly reduced. When a super module is turned off, other super modules continue working but share a higher voltage at ports at ⓓ, causing a deteriorated working condition. The power-circulation issue among primary modules is avoided due to the super module scheme. There is no medium ac voltage, hence the synchronization issue is avoided. Output ports of secondary modules share MVDC voltage.

PPDS: ① Ports at ⓐ and ⓑ are parallel simultaneously; primary modules are in an input-parallel-output-parallel connection, which produces a common ac bus at ⓑ. Hence the number of primary modules can be different from that of transformers, which increases the freedom of the transformer design. When a primary module is turned off by fault, other parts of the system still work normally. However, the parallel connection at ⓑ can lead to active and reactive power circulation between primary modules, which requires synchronization of PWM among modules and circulation-suppressing control or topology. A distributed synchronization scheme goes against transformers working at high frequency. Lower frequency leads to larger size and weight of the transformer and other passive components in the ac part, but benefits utilization of switches of larger power and voltage, e.g., IGBT. ② There is no medium ac voltage. Secondary voltage of each transformer is rectified by its exclusive secondary module; outputs of secondary modules at ⓓ are series to share the MVDC voltage, which brings low voltage stress.

3 System solutions

An existing system solution of PDSR, a solution of PPDS, and the proposed solution of PDDS are compared and evaluated through detailed qualitative and quantitative analysis. There is still no solution of PPSR, thus only the three solutions are presented.

3.1 System solution of PDSR

A solution of PDSR is shown in Fig. 5. It was originally designed for MVDC distribution networks to connect low and medium voltage dc-link [17]. This paper discusses the application of that solution in the dc grid-connected PV systems. Based on the parameters above, the number of primary modules is selected as n=10, and the number of MMC modules in an upper (and down) leg is selected as m=10.

At the low-voltage side, the modular isolated dc-ac converters are implemented by the full-bridge topology with a medium-frequency transformer. At the high-voltage side, a two-phase modular multi-level converter (MMC) is employed as the rectifier. MMC features good fault-tolerant capability due to module

redundancy. But it lacks the ability of soft-switching, which lowers the conversion efficiency. Full use of active switches brings flexible controllability and high power density, at the price of a higher device cost and complex control system.

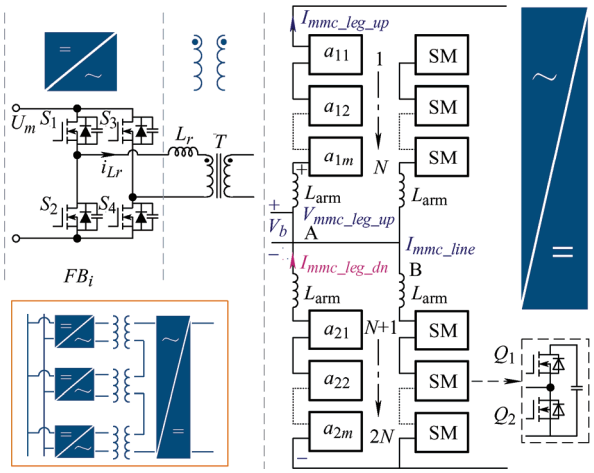

Fig. 5 Topology of PDSR system solution

Multilevel triangular voltage waves are modulated by both the primary and secondary sides, and a simple phase-shifting control is used to regulate power delivered by transformers. Fig. 6 shows the switching process during a PWM cycle.

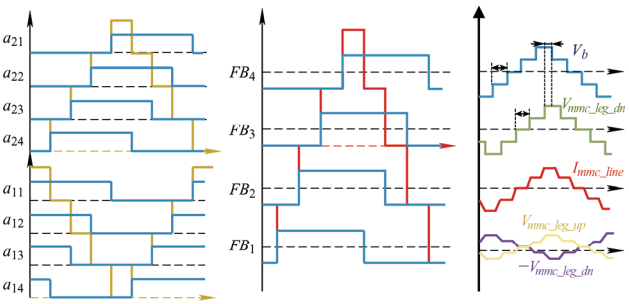

(a) PS modulation in MVDC side (b) PS modulation in LVDC side (c) PS modulation in MHFL

Fig. 6 Working principle of the solution of PDSR

For the shifted phase β between V_{mmc_leg} and V_b, in a range of $\beta \in [-\frac{\pi}{2}, \frac{\pi}{2}]$, power delivered from the primary side to the secondary side increases with increasing β.

A highly centralized PWM generator is required to guarantee all modulation in both full bridges and MMC is synchronized. When the voltage of PV arrays varies, the duty cycle control must be involved [18-20]. But PWM will surely be much more complicated to realize. Besides, as shown in Fig. 6, different full bridges output different currents when they modulate a square voltage wave, which causes unequal active and reactive power. A method to deal with this problem is that carriers may take turns to serve each full bridge modulation, so as to achieve circulant average power sharing, at the price of higher modulation complexity. A similar problem exists in the MMC converter, and it must be coped with.

In addition, the loss models of each part of the system solutions are summarized as follows.

Conduction loss of the switching device

$$P_c = I_{s,rms}^2 R_{ds,on} \tag{1}$$

Switching loss of the switching device

$$P_s = \frac{1}{2} V_{ds} I_{ds} \left(t_r + t_f\right) f_s \tag{2}$$

Conduction loss of the inductor

$$P_l = I_{l,rms}^2 R_{lr} \tag{3}$$

Conduction loss of the diode

$$P_d = V_f I_f \tag{4}$$

According to the above models, the loss and efficiency of the three system solutions can be compared and analyzed.

3.2 System solution of PDDS

A solution of PDDS is proposed by the authors and shown in Fig. 7. Each modular dc-dc converter is realized by the four-phase interleaved Boost converter at the front stage and the three-level LLC converter as the back stage.

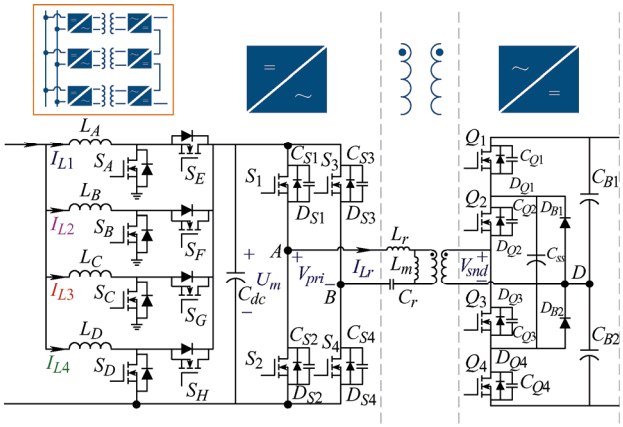

Fig. 7 Topology of PDDS system solution

The interleaved Boost converter and LLC converter form a super module. The Boost converter is the simplest converter, and it has considerable efficiency. The interleaved structure reduces the inductance and current demand of a single inductor. The Boost converter converts the variant voltage of

PV arrays to a constant voltage on C_{dc}. Hence the LLC converter can work with a fixed voltage gain, allowing it to work at its resonant frequency with open loop control and maximized efficiency. For further voltage-stress reduction and higher voltage gain on the primary side, an NPC three-level half-bridge is utilized as the secondary module in the LLC converter.

The working principle of an interleaved Boost converter is shown in Fig. 8a. By using a fixed phase shift among carriers of four parallel single Boost converters, the total current ripple of all single Boost converters is much less than that of a single one. Both the primary and secondary sides of the LLC converter modulate 50% duty cycle square voltage waves to the resonant tank and transformer. There is no phase lag between square voltages of the primary and secondary sides. The NPC three-level half-bridge is operated with specialized switching to facilitate dead-band control, as seen in Fig. 8b.

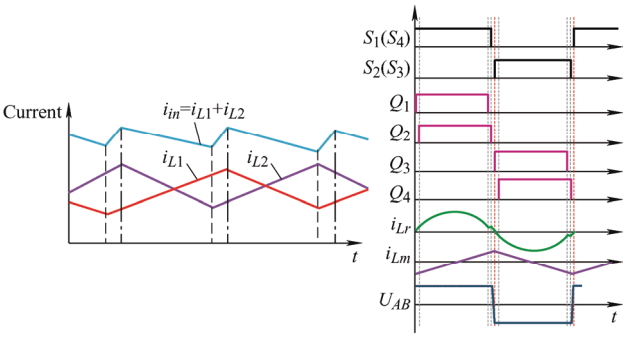

(a) Reduced current ripples of interleaved Boost converters (b) Three-level NPC LLC converter in resonant frequency

Fig. 8 Working principle of the solution of PDDS

Control of the solution of PDDS is very simple. Only the duty cycle of the Boost converter is used to regulate the input power. There is no PWM synchronization issue among super modules, hence each has a modular control system, and they only need to share a current dispatch from a superior controller. Open-loop control for the LLC converter significantly simplifies the sampling and control on the MVDC side, which greatly benefits insulation design. The combination of Boost and LLC converters leads to the highest efficiency among the compared solutions. However, for a PDDS system, once a fault occurs to stop any sub-module of a super module, the super module must be turned off, and other super modules must take its voltage share on the output port, causing a deteriorated working condition. The full active-switch design of the solution of PDDS increases the incidence of such faults.

3.3 System solution of PPDS

The solution of PDDS is shown in Fig. 9 [21]. A three-phase voltage source converter (VSC) is employed as the primary module. Phase-shift transformers work in low frequency. A three-phase diode rectifier is the secondary module. This solution comes from a LCL boosting idea [22-23].

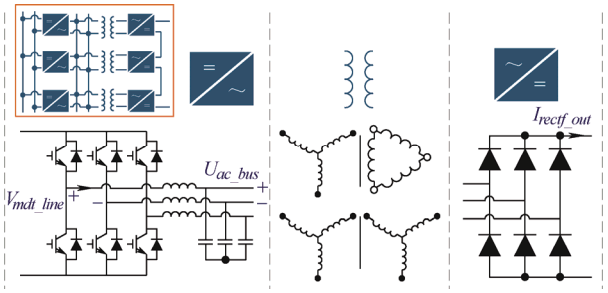

Fig. 9 Topology of PPDS system solution

The VSC module converts voltage of PV arrays to switching ac voltage with a low-frequency fundamental component. With the LC filter, the fundamental component is magnified five times and the high-frequency harmonics are filtered out. By parallel connection, an ac bus appears on the primary side of transformers. Each secondary module rectifies the ac voltage of its exclusive transformer, and the dc outputs are series-connected to produce medium dc voltage, which is integrated with the MVDC grid.

To reduce input power fluctuation and increase power density, a three-phase scheme is used for the modules. Sinusoidal PWM is utilized for VSC, as shown in Fig. 10. There are nearly no low-order harmonics, hence the voltage at the ac bus is quite sinusoidal. The modulation ratio is the only control variable, and it adapts to variant input voltage, which benefits the MPPT of PV arrays. Due to the ac bus, modulations of each primary module must be synchronized; a centralized PWM generator is preferred. But, since the ac bus works at a low frequency, a distributed synchronization scheme is also suitable, such as virtual synchronous generator control [24-25]. The low working frequency of the ac part dramatically increases the size and weight of passive components like capacitors and inductors. The LC filters magnify the fundamental component at the

price of large reactive power, which reduces efficiency when the PV power is low. The diode rectifier is very simple and reliable, which avoids sampling and control issues on the medium-voltage side, and has the easiest insulation design requirement of all solutions. To reduce current ripples caused by diode rectifiers, the transformers are selected to be 30° phase-shifting pairs, so as to realize 12-pulse rectification. For a PPDS system, the number of primary modules can be different from that of the transformers, and if a primary module is turned off, other parts of the system can still work normally, hence the solution of PPDS is particularly suitable to set up standby primary modules. Owing to the high reliability of transformers and diode rectifiers, the solution of PPDS features a good ability to continue working during a fault, which is significant for large-power generation.

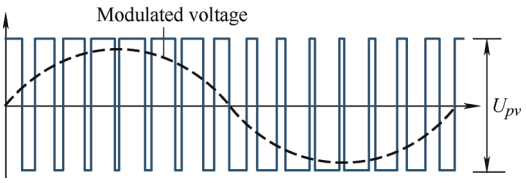

Fig. 10 Modulation in three-phase VSC

4 Performance and cost comparison of the solutions

To facilitate a fair comparison, the main parameters of the three system solutions are input voltage range 400-900 V (PV MPPT), output voltage range ± 10 kV, and rated power 1 MW. The circuit models of these three systems based on typical topologies are built in Matlab/ Simulink. Power-loss models are also established. The input/intermediate/ output voltage/current performances are tested and compared based on circuit simulations. The conversion efficiency and power-loss distribution are investigated and evaluated. Power density, efficiency, and hardware cost of these three solutions are studied and compared.

The PV arrays are simulated by dc source, inner resistance, and parallel capacitors, similar to the MVDC side, as shown in Fig. 11.

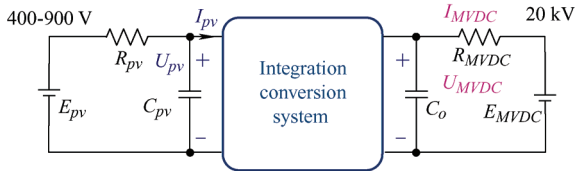

Fig. 11 PV and MVDC simulated interfaces

Based on the parameters above, the number of each kind of module of the three solutions is selected and listed in Tab. 1. For Solution of PDSR, the number of secondary modules refers to the number of sub-modules in an upper leg of the MMC rectifier. Since the power of a three-phase full-bridge system is $\sqrt{3}$ times that of a single-phase full-bridge system, the basic number of modules in the solution of PPDS is selected as $10/\sqrt{3} \approx 6$.

Tab. 1 Module numbers

Parameter	Solution of PDSR	Solution of PDDS	Solution of PPDS
Primary modules *m*	10	10	6
Transformers *w*	10	10	6
Secondary modules *n*	10 (MMC)	10	6
Constraint	*m*=*w*	*m*=*w*=*n*	*w*=*n*

Circuit simulations in Matlab/Simulink are conducted with the parameters in Tab. 2. The detailed parameter design process of Solution of PDSR and the solution of PPDS can be found in Refs. [17-21] respectively.

Tab. 2 Parameter design

Solution	Item	Value
Solution of PDSR	Frequency (FB)/kHz	100
	Frequency (MMC)/kHz	100
	Transformer ratio	1:3.2
	C_{pv}/μF	80
	L_{arm}/μH	216
	C_{ij}/μF	5
	C_o/μF	250
Solution of PDDS	PWM frequency	100 kHz (Boost) 100 kHz (LLC)
	Transformer ratio	1:1
	C_{pv}/μF	80
	L_A= L_B= L_C= L_D	198 μH
	C_m/μF	350
	L_m/μH	197
	L_r/μH	16.4
	C_r/nF	68.5
	C_{ss}/μF	5
	C_{B1}= C_{B2}	120 μF
	C_o/μF	167
Solution of PPDS	PWM frequency/kHz	100
	AC bus frequency/Hz	1 250
	LC step-up ratio	1:5
	Transformer ratio	1:1.67
	C_{pv}/μF	80
	L/μH	349
	C/μF	41.7
	L_{leak}/μH	10
	C_o/μF	167

4.1 Dynamic response

The simulated response-performance test is

guided in open-loop control to reveal the inherent features of the solutions. Note that closed-loop control strategies but can be realized with the aforementioned control variables, but are not presented in this paper. Each solution is tested in two situations: ① The critical voltage and current waves in several steady cycles are presented to show and verify their working principles under full power output; ② In a much longer time scale, the control variable of each solution steps away and back to let the system work from full power to half power, and then back to full power, to show its potential response in terms of speed and oscillation.

4.1.1 The solution of PDSR

As shown in Fig. 12, the MMC line current is very smooth due to a high number of voltage levels.

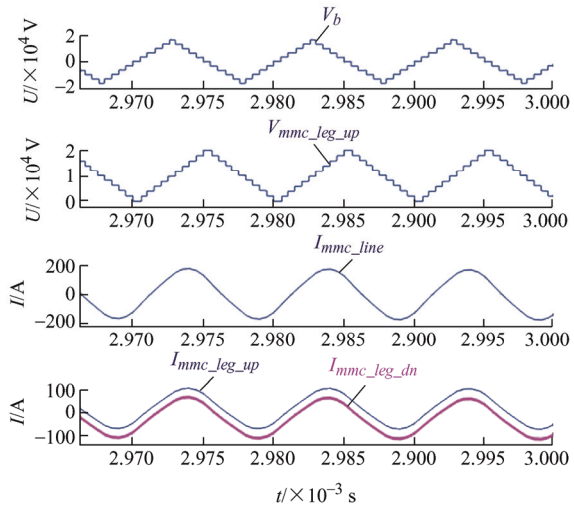

Fig. 12 Cycle waves in steady state of the solution of PDSR

Shifting-phase β is the control variable. As shown in Fig. 13, the system responds quickly with little overshoot due to the DAB scheme, which has few passive-energy storage components.

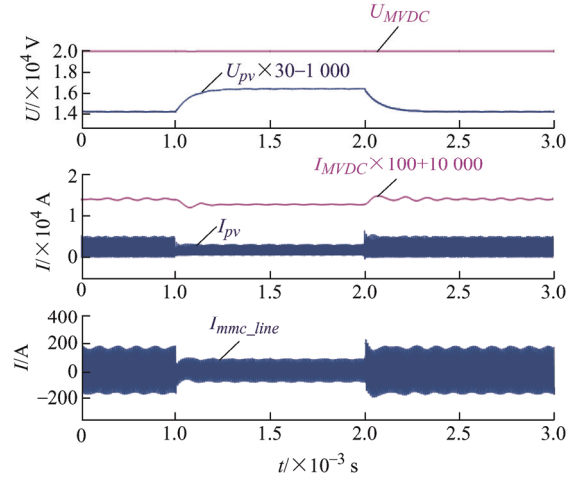

Fig. 13 Power step response of the solution of PDSR

4.1.2 The solution of PDDS

As shown in Fig. 14, currents of interleaved Boost converters mitigate the total ripples. The LLC converters always work in a resonant frequency for high efficiency.

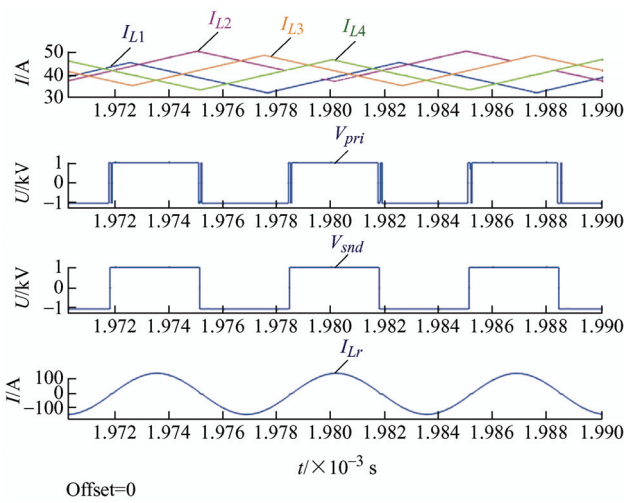

Fig. 14 Cycle waves in steady state of the solution of PDDS

The duty cycle of Boost converters is the control variable. As shown in Fig. 15, though the LLC converter responds quickly, the system response speed is still lower, owing to the Boost inductors and intermediate capacitors linking Boost converters and the LLC converter.

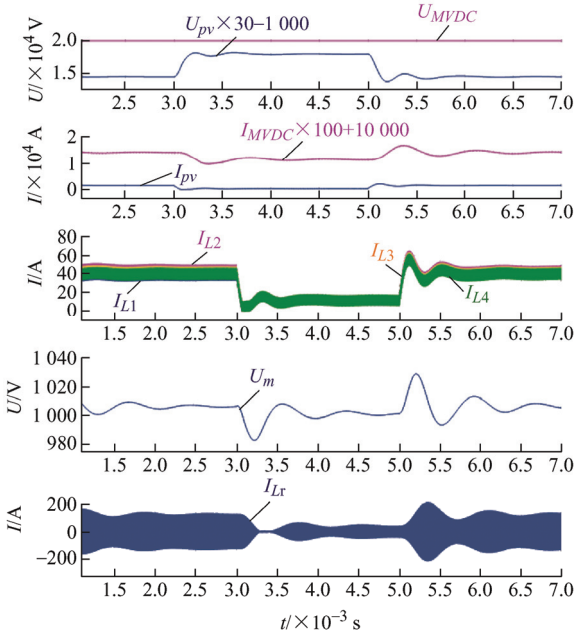

Fig. 15 Power step response of the solution of PDDS

4.1.3 The solution of PPDS

As shown in Fig. 16, the modulated voltage by VSC is well filtered, and the fundamental components are magnified to facilitate a high voltage step-up ratio.

The 12-pulse rectification on the secondary side greatly reduces power ripples.

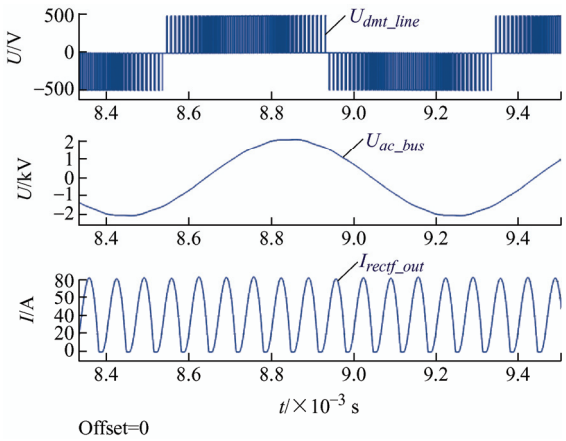

Fig. 16 Cycle waves in steady state of the solution of PPDS

The modulation ratio of VSC is the control variable. As shown in Fig. 17, the response speed of this solution is slowest, since it is a low-frequency design with large LC filters and passive rectifiers on the secondary side.

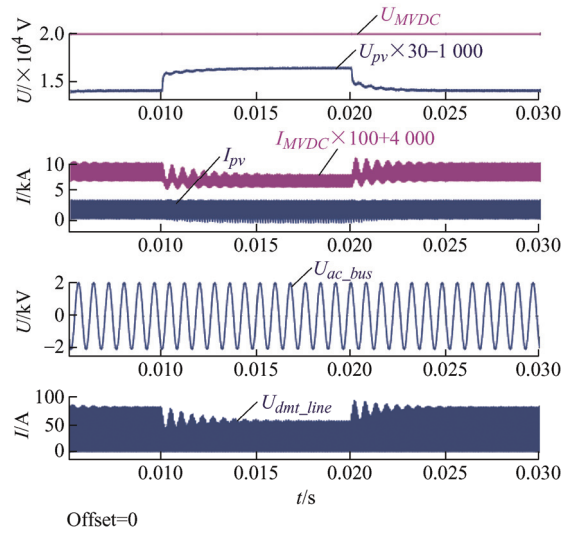

Fig. 17 Power step response of the solution of PPDS

4.2 Hardware cost of power circuit

To enhance the efficiency of the solutions, SiC MOSFETs and diodes are widely used in device selection. The approximate costs for main hardware of power circuit in each solution are presented in Tabs. 3-5. The solution of PDDS costs most due to many more passive components and active switches used than other two. The solution of PDSR and PPDS are similar in total price. The solution of PDSR has less inductors and capacitors, but more switches; while the solution of PPDS has more inductors and capacitors, but less switches.

Tab. 3 Main hardware cost of the solution of PDSR

Components	Model	Number	Cost/(¥/each)
FB switch $S_{1\text{-}4}$	C2M0025120D	10×3×4	430
MMC switch $Q_{1\text{-}2}$	C2M0045170D	4×20	580
PV capacitor C_{pv}	MKP1848C62012JY5	20 μF×40	155
MMC module cap C_{ij}	MKP1848C55012JK2	4×5 μF×40	47
MMC arm inductor L_{arm}	Ferrosilicon (core)	4	1 000
Tranformer T	Ferrite	10	12 000
Total cost: 230 080 ¥ ≈ 36.5k $			

Tab. 4 Main hardware cost of the solution of PDDS

Components	Model	Number	Cost/(¥/each)
Boost switch S_A	C2M0045170D	10×2×4	580
Boost diode S_E	C2M0045170D	10×2×4	580
LLC pri switch $S_{1\text{-}4}$	C2M0045170D	10×2×4	580
LLC snd switch $Q_{1\text{-}4}$	C2M0045170D	10×4	580
LLC snd diode $D_{B1\text{-}2}$	C2M0045170D	10×2	580
PV input capacitor C_{pv}	MKP1848C62012JY5	4×20 μF×10	155
Intermediate capacitor C_m	MKP1848C62012JY5	16×20 μF×10	155
	MKP1848C55012JK2	6×5 μF×10	47
	716P472916L	4×4.7 nF×10	36
Flying capacitor C_{ss}	MKP1848C55012JK2	4×5 μF×10	47
Three-level capacitor $C_{B1\text{-}2}$	MKP1848C62012JY5	6×20 μF×10	155
	716P473912M	2×47 nF×10	33
Boost inductor $L_{A\text{-}D}$	Ferrosilicon (core)	10×4	1 000
Resonant capacitor C_r	716P333920M	8×33 nF×10	151
Transformer T (L_r, L_m)	Ferrite (core)	10	12 000
Total cost: 393 180 ¥ ≈ 62.3k $			

Tab. 5 Main hardware cost of the solution of PPDS

Components	Model	Number	Cost/(¥/each)
VSC switch $S_{1\text{-}6}$	C2M0025120D	6×4×6	430
Diode rectifier $Q_{1\text{-}6}$	VSSD263C45S50L	6×6	1 109
PV capacitor C_{pv}	MKP1848C62012JY5	20 μF×40	155
LC filter capacitor C	MKP1848C63012JY5	3×6×30 μF	159
LC filter inductor L	Ferrosilicon (core)	3×6	2 200
Transformer T (L_r, L_m)	Nanocrystalline (core)	6	10 000
Total cost: 253 184 ¥ ≈40.1k $			

4.3 Conversion efficiency

Approximate estimation of power loss are listed in Tab. 6. Due to the soft switching capability of LLC converter, the solution of PDDS features highest

system efficiency. Efficiency of the solution of PDSR is suffered from large reactive power. Efficiency of the solution of PPDS is suffered from both reactive power and diode voltage drop.

Tab. 6 Estimated power loss of three solutions

Solutions	Item	Loss/W	Efficiency(%)
Solution of PDSR	Primary full bridges	6 708	≈ 97.8
	MMC switch	11 472	
	Transformers	2 520	
	Inductors	1 323	
	Total	22.0×10^3	
Solution of PDDS	Boost switch	1 979	≈ 99.4
	LLC primary full bridges	990	
	LLC secondary half bridges	706	
	Transformers	2 370	
	Inductors, capacitors	822	
	Total	6.05×10^3	
Solution of PPDS	VSC switch	5 190	≈ 98.6
	Diode	2 854	
	Transformer	3 214	
	Inductors, capacitors	2 562	
	Total	13.8×10^3	

The loss distribution ratio diagram of each solution is shown in Fig. 18. In each solution, the conduction loss and switching loss of switching devices still occupy the largest proportion.

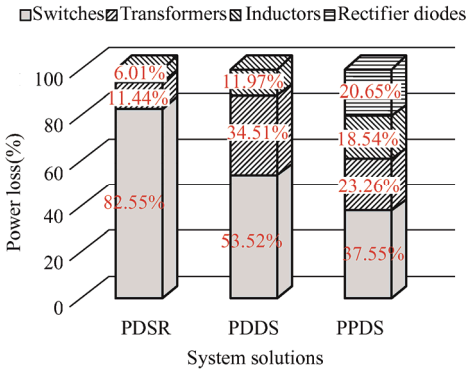

Fig. 18 The loss distribution ratio diagram of the three solutions

The actual loss distribution diagram of the three solutions is shown in Fig. 19. It can be seen from the vertical comparison that the design of the PDDS solution effectively reduces the loss on the switching devices.

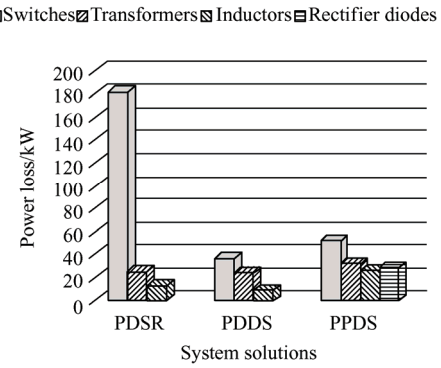

Fig. 19 The actual loss distribution diagram of the three solutions

4.4 Summary

With the evaluation summarized in Tab. 7, the most suitable solutions for large-capacity PV generation integrated into an MVDC grid are the solution of PDDS and the solution of PPDS.

Tab. 7 Summary of comparisons

System solutions	PDSR	PPSR	PDDS	PPDS
Modular design	low	low	very high	high
Suitability for MPPT of PV	medium	high	very high	very high
Distributed PWM generator	low	medium	very high	high
Fast response	very high	low	high	low
Simple sampling & control	low	high	very high	very high
Less inner reactive power	low	medium	very high	high
Less use of active switches	low	high	low	very high
Frequency of transformer	high	low	very high	low
Fault ride-through ability	medium	high	medium	very high
Independence of pri & snd	high	high	low	high
Conversion efficiency	low	medium	very high	medium
Power density	high	low	very high	low
Less device cost	high	medium	low	medium
Applicability	medium	high	very high	very high

5 Conclusions

In this paper, the emerging conversion systems for large-scale PV plants integrated into MVDC grid are studied. The required structural features for such a conversion system are discussed. The conversion system can be classified into four categories by series-parallel connection scheme of power modules: PDSR, PPSR, PDDS and PPDS. Features of each connection-scheme are qualitatively analyzed. A solution of PDDS is also proposed in this paper.

Through comparison of the proposed solution with the existing solutions of PDSR and PPDS are conducted through module topology analysis, simulation verification, and estimates of efficiency and cost.

The system-connection schemes PDDS and PPDS are most promising. Usually, the PDDS scheme leads to high PWM frequency, good response, high power density and high efficiency, but it has a high cost for active switches and has common reliability. On the other hand, the PPDS scheme leads to low PWM frequency, slow response, low power density, and common efficiency. But it has a low cost of active switches and is highly reliable.

References

[1] A Q Huang, M L Crow, G T Heydt, et al. The future renewable electric energy delivery and management (FREEDM) system: The energy internet. *Proceedings of the IEEE*, 2011, 99(1): 133-148.

[2] E Rodriguez-Diaz, J C Vasquez, J M Guerrero. Intelligent dc homes in future sustainable energy systems: When efficiency and intelligence work together. *IEEE Consumer Electronics Magazine*, 2016, 5(1): 74-80.

[3] M Starke, L M Tolbert, B Ozpineci. AC vs. DC distribution: A loss comparison. *2008 IEEE/PES Transmission and Distribution Conference and Exposition*, 2008, Chicago, IL, USA.

[4] M Ding, Z Xu, W Wang, et al. A review on China's large-scale PV integration: Progress, challenges and recommendations. *Renewable and Sustainable Energy Reviews*, 2016, 53(9): 639-652.

[5] F Li, C Li, K Sun, et al. Capacity configuration of hybrid CSP/PV plant for economical application of solar energy. *Chinese Journal of Electrical Engineering*, 2020, 6(2): 19-29.

[6] P A Basore, D Chung, T Buonassisi. Economics of future growth in photovoltaics manufacturing. *2015 IEEE 42nd Photovoltaic Specialist Conference (PVSC)*, 2015, New Orleans, LA, USA.

[7] D Jiang, H Zheng. Research status and developing prospect of dc distribution network. *Automation of Electric Power Systems*, 2012, 36(8): 98-104.

[8] B Subudhi, R Pradhan. A comparative study on maximum power point tracking techniques for photovoltaic power systems. *IEEE Transactions on Sustainable Energy*, 2013, 4(1): 89-98.

[9] L Zhang, F Jiang, D Xu, et al. Two-stage transformerless dual-buck PV grid-connected inverters with high efficiency. *Chinese Journal of Electrical Engineering*, 2018, 4(2): 36-42.

[10] P S Shenoy, K A Kim, B B Johnson. Differential power processing for increased energy production and reliability of photovoltaic systems. *IEEE Transactions on Power Electronics*, 2013, 28(6): 2968-2979.

[11] W Chen, X Ruan, H Yan, et al. DC/DC conversion systems consisting of multiple converter modules: Stability, control, and experimental verifications. *IEEE Transactions on Power Electronics*, 2009, 24(6): 1463-1474.

[12] J W Kim, J S You, B H Cho. Modeling, control, and design of input-series-output-parallel connected converter for high-speed-train power system. *IEEE Transactions on Industrial Electronics*, 2000, 48(3): 536-544.

[13] Y Huang, C K Tse. Circuit theoretic classification of parallel connected dc-dc converters. *IEEE Transactions on Circuits and Systems I: Regular Papers*, 2007, 54(5): 1099-1108.

[14] N Eghtedarpour, E Farjah. Distributed charge/discharge control of energy storages in a renewable-energy-based DC micro-grid. *IET Renewable Power Generation*, 2014, 8(1): 45-57.

[15] W Li, X Lü, Y Deng, et al. A review of non-isolated high step-up dc/dc converters in renewable energy applications. *2009 Twenty-Fourth Annual IEEE Applied Power Electronics Conference and Exposition*, 2009, Washington, DC, USA.

[16] W Wu, Y He, P Geng, et al. Key technologies for dc micro-grids. *Transactions of China Electrotechnical Society*, 2012, 27(1): 98-106, 113.

[17] B Zhao, Q Song, J Li, et al. Modular multilevel high-frequency-link dc transformer based on dual active phase-shift principle for medium-voltage dc power distribution application. *IEEE Transactions on Power Electronics*, 2017, 32(3): 1779-1791.

[18] H Bai, Z Nie, C C Mi. Experimental comparison of traditional phase-shift, dual-phase-shift, and model-based control of isolated bidirectional dc-dc converters. *IEEE Transactions on Power Electronics*, 2010, 25(6): 1444-1449.

[19] F Krismer, J W Kolar. Closed form solution for minimum conduction loss modulation of dab converters. *IEEE*

Transactions on Power Electronics, 2012, 27(1): 174-188.

[20] V Karthikeyan, R Gupta. FRS-DAB converter for elimination of circulation power flow at input and output ends. *IEEE Transactions on Industrial Electronics*, 2018, 65(3): 2135-2144.

[21] M Li, Z Xie, L Yao, et al. Cascaded LC-AC transformer unidirectional DC-DC converter with high stepping ratio. *Transactions of China Electrotechnical Society*, 2017, 32(24): 1-9.

[22] D Jovcic, L Zhang. LCL DC/DC converter for DC grids. *IEEE Transactions on Power Delivery*, 2013, 28(4): 2071-2079.

[23] D Jovcic, W Lin. Multiport high power LCL DC hub for use in DC transmission grids. *2014 IEEE PES General Meeting | Conference & Exposition*, 2014, National Harbor, MD, USA.

[24] M Torres, L A C Lopes. Virtual synchronous generator control in autonomous wind-diesel power systems. *2009 IEEE Electrical Power & Energy Conference (EPEC)*, 2009, Montreal, QC, Canada.

[25] Q C Zhong, G Weiss. Synchronverters: Inverters that mimic synchronous generators. *IEEE Transactions on Industrial Electronics*, 2011, 58(4): 1259-1267.

Shilei Lu (S'18) received the B.E. degree in Electrical Engineering from Southwest Jiaotong University, Chengdu, China, in 2017. He is currently a Ph.D. candidate in Department of Electrical Engineering, Tsinghua University, Beijing, China. His research interests include high efficiency DC-DC converters, multi-level converters, photovoltaic generation and micro-grid applications.

Kai Sun (M'12-SM'16) received the B.E., M.E., and Ph.D. degrees in Electrical Engineering from Tsinghua University, in 2000, 2002, and 2006, respectively. He joined the Faculty of Electrical Engineering, Tsinghua University, in 2006, where he is currently a Tenured Associate Professor (Research Professor). From Sep. 2009 to Aug. 2010, he was a Visiting Scholar at Department of Energy Technology, Aalborg University, Aalborg, Denmark. From Jan. to Aug. 2017, he was a Visiting Professor at Department of Electrical and Computer Engineering, University of Alberta, Edmonton, Canada. His research interests include power electronics for renewable generation systems, microgrids, and energy internet, high performance converters for hybrid AC/DC microgrids, power quality and distributed power generation system.

Dr. Sun serves as an Associate Editor for IEEE Transactions on Power Electronics, IEEE Journal of Emerging and Selected Topics in Power Electronics, and Journal of Power Electronics. Dr. Sun served as the TPC Vice Chair of IEEE ECCE 2017 and IEEE ECCE-Asia 2017, the Organization Committee Chair of IEEE eGrid 2019, and the Publicity Chair of IEEE ECCE 2020. He also served as the General Co-Chair of 2018 International Future Energy Challenge (IFEC 2018). Dr. Sun serves as PELS Asia Pacific Regional Vice Chair, PELS Beijing Chapter Chair and PELS Electronic Power Grid Systems Technical Committee (TC8) Secretary. He was a recipient of Delta Young Scholar Award in 2013, and Youth Award of China Power Supply Society (CPSS) in 2017, and IEEE Transactions on Power Electronics' Outstanding Reviewers Award in 2019. Dr. Sun is selected as IEEE PELS Distinguished Lecturer in 2021-2022.

Haixu Shi (S'16) received his bachelor's degree in 2014 and his Ph.D. in 2020, both of Electrical Engineering from Tsinghua University, Beijing, China. His current research interests include modeling and control of DC-DC and AC-DC interlinking converters in microgrid applications. He is a reviewer of Journal of Power Electronics, and IEEE Transactions on Power Electronics.

Yunwei Li (S'04-M'05-SM'11) received the B.Sc. in Engineering degree in Electrical Engineering from Tianjin University, Tianjin, China, in 2002, and the Ph.D. degree from Nanyang Technological University, Singapore, in 2006.

In 2005, Dr. Li was a Visiting Scholar with Aalborg University, Denmark. From 2006 to 2007, he was a Postdoctoral Research Fellow at Ryerson University, Canada. In 2007, he also worked at Rockwell Automation Canada before he joined University of Alberta, Canada in the same year. Since then, Dr. Li has been with University of Alberta, where he is a Professor now. His research interests include distributed generation, microgrid, renewable energy, high power converters and electric motor drives.

Dr. Li serves as Editor-in-Chief for IEEE Transactions on Power Electronics Letters. Prior to that, he was Associate Editor for IEEE Transactions on Power Electronics, IEEE Transactions on Industrial Electronics, IEEE Transactions on Smart Grid, and IEEE Journal of Emerging and Selected Topics in Power Electronics. Dr. Li received the Richard M. Bass Outstanding Young Power Electronics Engineer Award from IEEE Power Electronics Society in 2013 and the second prize paper award of IEEE Transactions on Power Electronics in 2014.

Guoen Cao received the B.S degree in Electrical Engineering from Shandong University of Science and Technology, Qingdao, China, in 2009, the M.S. degree in Electrical Engineering from Beihang University, Beijing, China in 2012, and the Ph.D. degree in Electronics System Engineering from Hanyang University, Seoul, Korea in 2015. He is currently an Assistant Professor of Institute of Electrical Engineering, Chinese Academy of Sciences. His current research interests include resonant and soft switching power converter design, high efficiency power supplies in renewable energy applications, wide bandgap semiconductors and application, and electric vehicles.